Tsinghua University
Academic Works
清华大学学术专著

Multi-Phase Chemical Reaction Engineering and Technology (Part II)

多相化学反应工程与工艺(下)

Editors: Yong JIN, Fei WEI
金 涌　魏 飞　主编

Tsinghua University Press
清华大学出版社

Tsinghua University
Academic Works
清华大学学术专著

Multi-Phase Chemical Reaction Engineering and Technology (Part II)

多相化学反应工程与工艺(下)

Editors: Yong JIN, Fei WEI
金涌　魏飞　主编

Tsinghua University Press
清华大学出版社

4 Liquid-Solid, Gas-Liquid and Gas-Liquid-Solid Multi-Phase Reactors

4.1 Fundamental studies

4.1.1 Bed collapse technique for estimating parameters of generalized wake model for a three-phase fluidized bed

4.1.1.1 Introduction

The generalized wake model, developed by Bhatia and Epstein[1] to describe the hydrodynamic behavior of cocurrent three-phase fluidized beds, is widely accepted. With this model, the effect of the wakes behind gas bubbles on liquid flow can be mathematically formulated to elucidate bed expansion, particle entrainment and bed contraction.

The model considers the cocurrent upward gas-liquid-solid fluidized bed to be composed of a gas-bubble region, a wake region and a solid-liquid fluidization region, as shown in Fig. 1.

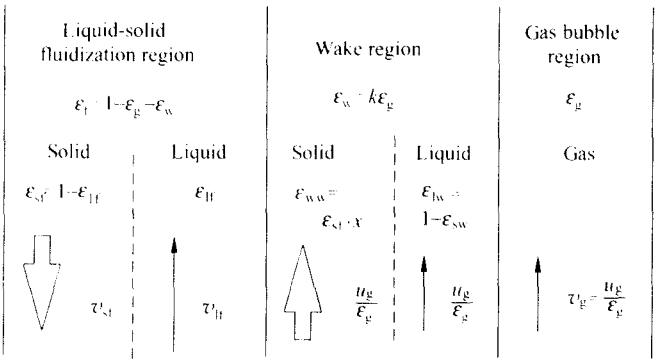

Fig. 1 Generalized wake model for a cocurrent upward three-phase fluidized bed

The model assumes that the liquid-solid relative velocity u_{lf} in the liquid-solid fluidization region can be related to the liquid hold-up ε_{lf} by the Richardson and Zaki equation[2]:

$$u_{lf} = u_t \varepsilon_{lf}^n \tag{1}$$

and that the wake moves up at the same velocity as the bubble. Two key parameters of the model (k and x) were defined:

$$k = \varepsilon_w / \varepsilon_g \tag{2}$$

$$x = \varepsilon_{sw}/\varepsilon_{sf} \tag{3}$$

The resultant expression for the liquid hold-up reads as follows:

$$\varepsilon_l = \left\{\left[u_l - u_g k(1-x)\right] \Big/ \left[u_i(1-\varepsilon_g - k\varepsilon_g)\right]\right\}^{1/n} \times\left[1-\varepsilon_g(1+k-kx)\right] + \varepsilon_g k(1-x) \tag{4}$$

where the values of k and x have to be estimated experimentally.

Based on the generalized wake model, however, one cannot determine the values of k and x from the hold-up data alone. Many investigators have tried to solve this problem.

For example, Bhatia and Epstein[1] presented an heuristic equation for k, assuming that the wake behavior in the three-phase system is analogous to that in a liquid-liquid dispersion:

$$k = \left[0.61 + 0.037/(\varepsilon_g + 0.013)\right]\varepsilon^3 \tag{5}$$

El-Temtamy and Epstein[3] obtained an expression for k_0 by assuming that a bubble and its wake form a complete sphere. Thus, the value of k can be calculated with the following equation:

$$k = k_0 \exp(-5.08\varepsilon_g) \tag{6}$$

and x can be computed from the hold-up data. Correlation for x was expressed as:

$$\left.\begin{aligned} x &= 1-0.877u_i/(u_g/\varepsilon_g - u_l/\varepsilon_l) \\ &\quad \text{for} \quad u_i/(u_g/\varepsilon_g - u_l/\varepsilon_l) \leqslant 1.14 \\ x &= 0 \quad \text{for} \quad u_i/(u_g/\varepsilon_g - u_l/\varepsilon_l) > 1.14 \end{aligned}\right\} \tag{7}$$

However, neither equation has as yet been verified by other researchers.

The objective of the present work is to estimate the parameters k and x by applying the bed collapse technique to three-phase fluidized beds, in particular for beds contracting on the introduction of gas.

4.1.1.2 Theoretical model

The bed collapse technique has been used successfully in the study of gas-solid fluidization. For a three-phase fluidized bed operated at steady state, the bed collapsing process, occurring when the air supply is suddenly cut off, is shown in Fig. 2. In the first stage ($0 \leqslant t \leqslant t_1$), the bed surface collapses very rapidly. This stage corresponds to the bubble escaping process and, in the second stage ($t_1 < t \leqslant t_2$) of the bed collapsing process, the voidage of the liquid-solid fluidization region of the three-phase bed gradually approaches that of particulate liquid-solid fluidization.

At the same superficial liquid velocity u_l, the solid hold-up in the liquid-solid fluidization region of a three-phase bed is larger than that in the particulate liquid-solid bed (for $0 < x < 1$), so that, in the second stage, the bed surface rises.

And finally, in the third stage ($t > t_2$), the bed process turns into steady particulate liquid-solid fluidization. The overall collapsing curve consists of three linear segments *AB*, *BC* and *CD*. Because the bubble escaping process and the transition to the particulate fluidized bed

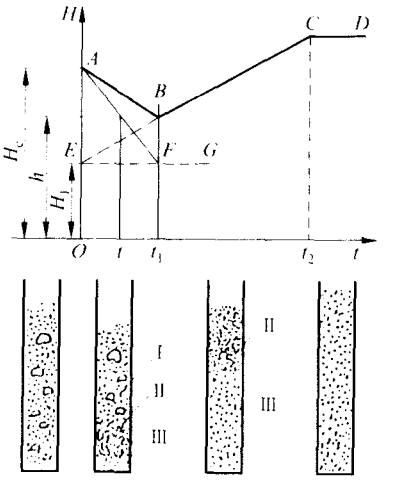

Fig. 2 Bed collapsing process by sudden interruption of air supply

I—three-phase fluidization region (original three-phase *FB*);

II—liquid-solid fluidization region after bubble escape (degassed three-phase *FB*);

III—particulate liquid-solid fluidization region (equilibrium L/S *FB*)

starts at the same time ($t = 0$), segment AB actually reflects the effects of both processes. The slope of segment BC represents the transition rate from liquid-solid fluidization region to particulate liquid-solid fluidized bed. Extending the line BC (broken line in Fig. 2) and crossing the vertical axis at E results in an intercept OE which corresponds to the height of a particulate fluidized bed containing all the solids at a liquid velocity u_{lf}. The horizontal line EG starting from point E crosses line t_1 B at point F. The slope AF is the average rate of the bubble escaping process.

In order to analyze the bed collapsing process in more detail, the following model is proposed as shown in Fig. 3.

Cross-sectional areas occupied by the liquid-solid fluidization region, the wake region and the gas-bubble region are A_f, kA_g and A_g respectively. Furthermore,

$$A_f + kA_g + A_g = A_T \tag{8}$$

where A_T is the total cross-sectional area of the bed. Since the gas-bubble and the wake are always combined together, a three-phase fluidized bed can be considered as two blocks (Fig. 3(a)).

After the air supply has been cut off, the original bubble-wake block still moves upwards at the same velocity (u_b), which can be considered as constant throughout the process of bed collapse. At time t, the bubble-wake block moves up through a distance h_1 (Fig. 3(b)):

$$h_1 = u_b t \tag{9}$$

At the same time, a volume of $(A_g + kA_g)h_1$ is vacated due to the rising bubble-wake block. This volume is taken up by the liquid-solid fluidization region, which reduces its height from H_c to h_2:

$$(H_c - h_2)A_f = (A_g + kA_g)h_1 \tag{10}$$

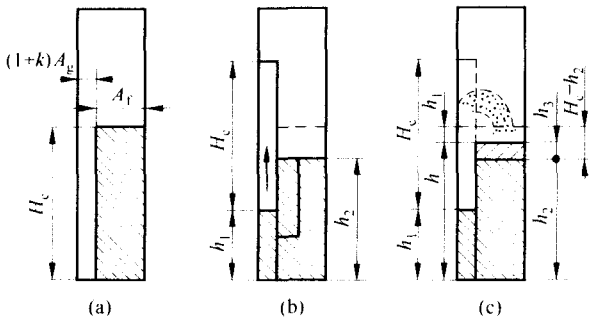

Fig. 3 Model of bubble escape and bed collapsing processes

Actually, when any part of the bubble-wake block reaches the bed surface, it breaks up. The solids contained in the wakes fall back and join the liquid-solid fluidization region (Fig. 3(c)).

At time t, the additional bed height caused by the falling back solids amounts to h_3, which can be determined from solid material balance for the wake solid sedimentation process:

Solids in the newly formed liquid-solid fluidization layer=Solids in the escaped wakes

$$h_3 A_f \varepsilon_{sf} = (H_c + h_1 - h_2 - h_3) A_g (kx) \varepsilon_{sf}$$
$$= [h_1 + (H_c - h_2) - h_3] kx \varepsilon_{sf} A_g \tag{11}$$

Eq. (11) can be transposed with respect to h_3:

$$h_3 = \left\{ kx u_b t \left[1 + (1+k) A_g / A_f \right] \right\} \Big/ \left[(A_f / A_g) + kx \right] \tag{12}$$

According to the above physical model, the relationships between the variables of a collapsing three-phase fluidized bed can be formulated.

(1) The instantaneous bed height h at time t during bed collapsing process is:

$$h = h_2 + h_3 \tag{13}$$

On applying Eqs. (10) and (12),

$$h = H_c - \left[A_g (1+k) u_b t \right] / A_f + \left\{ kx u_b t \left[1 + (1+k) A_g / A_f \right] \right\} / \left[(A_f / A_g) + kx \right] \tag{14}$$

where

$$\varepsilon_f + \varepsilon_g + \varepsilon_w = 1$$
$$u_b = u_g / \varepsilon_g = u_g (1+k) / (1 - \varepsilon_f)$$
$$A_f / A_g = \varepsilon_f / \varepsilon_g = \varepsilon_f (1+k) / (1 - \varepsilon_f)$$

Eq.(14) can be further transformed to

$$\varepsilon_f (1 + k - kx) + kx = [u_g (1+k)(kx - 1 - k)] / [(h - H_c)/t] \tag{15}$$

(2) Solid material balance in the original three-phase fluidized bed (t=0) can be expressed by:

Total solids in wakes +Total solids in liquid-solid fluidization region=Total solids in bed

$$A_T H_c \varepsilon_w \varepsilon_{sw} + A_T H_c \varepsilon_f \varepsilon_{sf} = \varepsilon_{s0} A_T H_0 \tag{16}$$

where

$$\varepsilon_{sw} = \varepsilon_{sf} x$$

$$\varepsilon_w = k(1-\varepsilon_f)/(1+k)$$

Eq. (16) can be transformed to

$$\varepsilon_{sf}[kx(1-\varepsilon_f)/(1+k)+\varepsilon_f] = \varepsilon_{s0} H_0 / H_c \tag{17}$$

(3) The balance of liquid volumetric flow rates in the bed can be expressed by:

Liquid volumetric flow rate in wakes + Liquid volumetric flow rate through liquid-solid fluidization region = Liquid volumetric flow rate at bed surface

$$\varepsilon_g k(1-x\varepsilon_{sf}) u_b A_T + \varepsilon_f u_{lf} A_T = u_l A_T \tag{18}$$

where u_{lf} can be calculated from the Richardson and Zaki Eq.(1), and $u_b = u_g/\varepsilon_g$.

Eq. (18) can be rearranged as follows

$$k u_g (1-x\varepsilon_{sf}) + \varepsilon_f u_i (1-\varepsilon_{sf})^n = u_l \tag{19}$$

(4) In Fig. 2, point E corresponds to a hypothetical operating condition under which all particles are fluidized at a liquid velocity u_{lf}. The solid material balance for this case is

Total solids in wakes + Total solids in liquid-solid fluidization region = Total solids in bed

$$H_c A_g k \varepsilon_{sw} + H_c A_f \varepsilon_{sf} = H_l A_T \varepsilon_{sf} \tag{20}$$

where

$$A_f = A_T \varepsilon_f, \quad \varepsilon_{sw} = \varepsilon_{sf} x, \quad A_g = A_T \varepsilon_g$$

Eq. (20) can be transformed into

$$(H_l / H_c) = \varepsilon_f + kx\varepsilon_g = \varepsilon_f + kx(1-\varepsilon_f)/(1+k) \tag{21}$$

Now there are four equations, namely Eqs. (15), (17), (19), (21) and four unknown parameters, k, x, ε_f, ε_{sf}, which can be determined from these equations by using the following experimental data:

u_l, u_g	operating conditions of experiments
H_c, H_l, H_0, t, h, ε_{s0}	experimental data measured during bed collapsing process
u_i, n	experimental data measured during bed expansion in liquid-solid fluidization

In the meantime, the relevant hold-up ε_g, ε_l and ε_s of the three-phase fluidized bed are defined as follows:

$$\left.\begin{aligned} \varepsilon_g &= (1-\varepsilon_f)/(1+k) \\ \varepsilon_s &= \varepsilon_f \varepsilon_{sf} + \varepsilon_g kx\varepsilon_{sf} \\ \varepsilon_l &= 1-\varepsilon_s-\varepsilon_g \end{aligned}\right\} \tag{22}$$

4.1.1.3 Experimental apparatus and method

A diagram of the experimental equipment is shown in Fig. 4. The vertical Perspex column is 0.050 m in diameter and 1.5 m in total height. The column consists of three sections, namely, the gas-liquid disengagement section, the test section, and the gas-liquid distributor section.

The distributor, located at the bottom of the test section, is designed according to Fan et al.[4]. The fractional free area of the distributor is 1.6%.

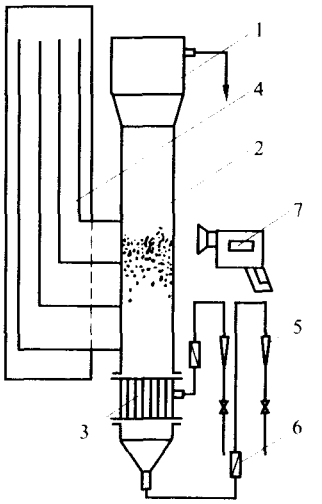

Fig. 4 Experimental set-up for the study of bed collapse process in a cocurrent gas-liquid-solid fluidized bed
1—gas-liquid disengagement section; 2—test section; 3—gas-liquid distributor section; 4—manometers; 5—rotameter; 6—solenoid valve; 7—video cassette recorder

Water and air were used in the experiments. In all experiments, the gas-liquid flow was cocurrent and directed upwards. Rotameters were used to measure the gas and liquid velocities, varying from 0 to 3.0 cm/s and from 3.0 cm/s to 5.5 cm/s respectively. Pressure taps were connected to water manometers or a mercury manometer for measurement of the static pressure profile along the column. Spherical glass bands, with an average diameter of 0.0011 m were used in the experiments and the height of the packed bed was 0.040 m.

The parameters, u_i and n, for the Richardson and Zaki equation of the given experimental system were measured in liquid-solid fluidized bed, giving $u_i = 0.1502$ m/s, $n = 2.56$, i.e.:

$$u_{lf} = 0.1502\varepsilon_{lf}^{2.56} \tag{23}$$

Under steady-state operation, bed collapse was produced by suddenly cutting off the flow of either just air or both air and liquid simultaneously (Fig. 5). The bed height was continuously monitored during the collapsing process with a video cassette recorder. Analysis of the video pictures frame by frame yielded two types of collapsing curves ($ABCD$ and $A'B'C'D'$) as shown in Fig.5.

The collapsing curve $ABCD$ corresponds to the sudden cut-off of the air supply, and $A'B'C'D'$ to simultaneous cut-off of both air and liquid supply. Both experimental results and theoretical analysis show that the time for complete escape of bubbles (t_1) is similar for the two types of transient behavior, for otherwise identical operating conditions (u_g, u_l, H_0). This has been inferred by extending the lines BC and $B'C'$ to the vertical axis and obtaining

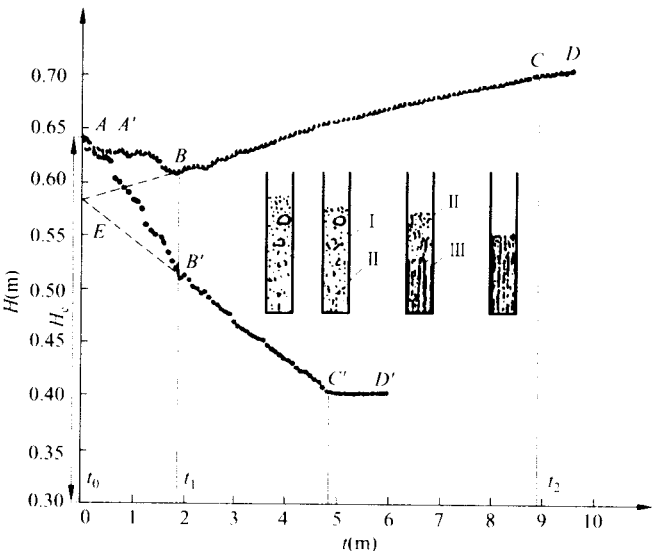

Fig. 5 Bed collapsing process on sudden interruption of both air and liquid supplies
(u_l = 0.043 m/s; u_g = 0.014 m/s)
I —three phase fluidization region; II —liquid-solid fluidization region after bubble escape;
III—settlement (sedimentation) region

similar intercepts (E) with the two types of induced transients.

4.1.1.4 Results and discussion

The variation of parameter k with superficial gas velocity, according to experimental results, is shown in Fig. 6(a). For a constant superficial liquid velocity, the increase of gas velocity in a three-phase fluidized bed leads to a decrease of parameter k.

For a constant gas velocity, the effect of the superficial liquid velocity on parameter k in a three-phase fluidized bed is shown in Fig. 6(b). In this case, increasing liquid velocity increases the value of k.

Experimental results also show that, under a constant superficial liquid velocity, parameter x increases with the initial increase in superficial gas velocities, as shown in Fig. 6(c).

Variation of parameter x with superficial liquid velocity is shown in Fig. 6(d). At a constant gas velocity, increasing superficial liquid velocity causes parameter x to decrease slightly.

For comparison with other investigations, the calculated values of k and x from Eqs. (5) to (7) were also plotted in Fig. 6.

In order to examine the feasibility of estimating the parameters of the generalized wake model in three-phase fluidized beds by using the bed collapse technique, the hold-up data, ε_s, ε_l and ε_g, were determined by measuring the pressure drops of the bed under the same operating conditions. The obtained hold-up data were compared with those predicted by the generalized wake model by using the parameters (k and x) estimated through the bed collapse technique. The results of comparison (Fig. 7) show that the agreement is quite good.

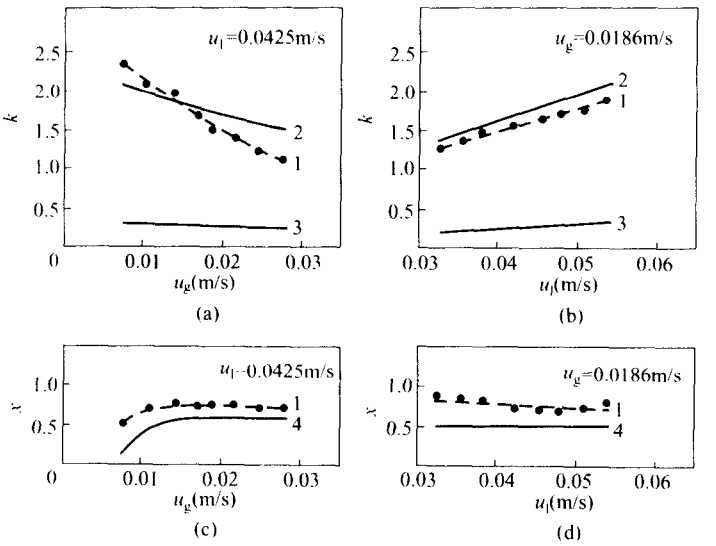

Fig. 6 Variations of k and x with gas and liquid velocities

---system air-water-0.0011 m dia. glass beads

1— experimental results by bed collapse technique; 2— calculated values of k using Eq.(6);

3— calculated values of k using Eq. (5); 4— calculated values of x using Eq. (7)

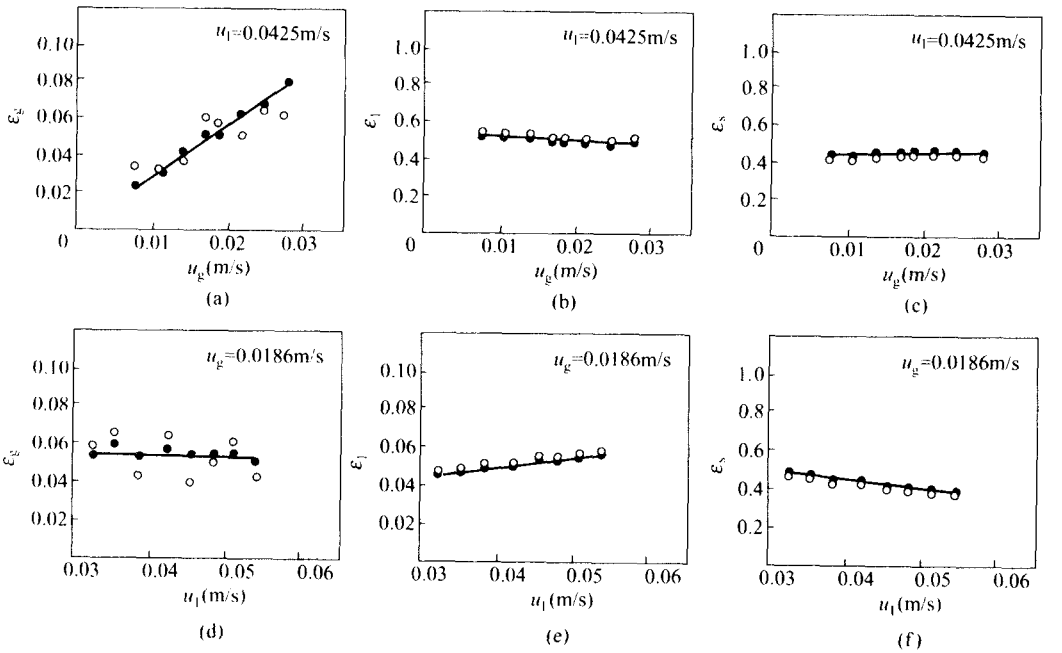

Fig. 7 Variations of solid,liquid and gas hold-ups with gas and liquid velocities

---system air-water-0.0011 m dia. glass beads; • by bed collapse method; ○ by pressure drop method

References

[1] Bhatia, V.K., Epstein, N., *Three Phase Fluidization: A Generalized Wake Model*, in: *Fluidization and its*

Applications (H. Angelino et al., Eds.), Cepadues-Editions, Toulose 1974, p.380-392.
[2] Richardson, J.F., Zaki, W.N., *Trans. Inst. Chem. Eng.*32 (1954) p. 35-52.
[3] El-Temtamy, S.A., Epstein, N., *Int. J. Multiphase Flow* (1978) No.4, p. 19-31.
[4] Fan, L.S., Muroyama, K., Chern, S.H., *Chem. Eng. J.(Lausanne)* 24(1982) p.143-150.

Above content refers to:

Jin Y., Zhang J. P., Yu Z. Q. Chem. Eng. Technol., 16 (1993): p.119-124

4.1.2 Application of Doppler ultrasound velocimetry in multiphase flow

4.1.2.1 Introduction

Multiphase flow reactors have been widely used in environmental, chemical and biochemical processes in last decades[6-8]. Although multiphase reactors are successfully and widely used in commercial industrial operations, much remains to be done due to the complexity of the multiphase flow. In order to gain fundamental knowledge about the complex multiphase flow behavior, research is still needed, and experimental work is obviously necessary. Measurement technique is very important in the study and design of multiphase systems and much work has been carried out in this field, but it is still a challenging research field[5,21].

Quantities needed to be measured in fluidized beds include local solid concentration, particle velocities, gas holdup, bubble behavior, liquid velocity, and their radial and axial profiles inside the system[21]. The solid distribution within the reactor greatly affects its performance[13]. Therefore the degree of dispersion of the solid (catalyst) in the reactor must be understood and controlled for the optimum design and operation of gas-liquid-solid three-phase reactors. The bubble behavior, one of the most important parameters for the reactor simulation and design, is related to the phase holdup, interphase drag and mass transfer behavior[19]. For better understanding of the multiphase flow, the local solid concentration and bubble parameters rather than spatial averaged values are needed. Computational fluid dynamics (CFDs) has been extensively investigated in multiphase flow simulation in the last two decades, while most of the models available for closure of the governing equations need the relative velocity between phases to model drag and non-drag forces[18]. This relative velocity is limited in literature due to the difficulty of velocity measurements in multiphase flow. Typically, the gas phase is measured and the relative velocity is determined through a drift flux correlation. Therefore, development of measuring the phase velocity simultaneously is a valuable work.

Extensive investigations have been carried out in developing measurement technique for multiphase flows[5,10], but there is still a great gap between the development and the requirement. Most measuring techniques reported in the literature are limited to single

parameter measurement, for example, reference[11] used a electrical conductivity probe to measure the solid concentration in the liquid-solid system. Yang et al.[24] used electrolyte tracer method to measure the local liquid velocity in a three-phase circulating fluidized bed (TPCFB)[17], used a hot wire probe to measure the local liquid velocity in the riser of an external loop airlift reactor[19,20], used a optic probe to measure the local gas holdup and bubble behavior in TPCFB, Vassallo et al.[18] used laser Doppler velocity (LDV) to measure the liquid and gas velocity, and Mudde et al.[12] reported on laser Doppler anemometer (LDA) experiments of measuring the liquid velocity field in a bubble column. Among these methods, electrolyte tracer method needs hundreds of tracer pulses and vast data acquisition, optic probe and hot wire are very fragile and need careful calibration, and LDV is expensive and only feasible in case of low solid and gas holdup. In recent years, ultrasound technique has drawn much attention as a non-intrusive and non-invasive measurement method due to its attractive advantages over the conventional techniques: ①an efficient flow mapping process; ②applicability to opaque systems; ③a record of the spatiotemporal velocity[15]. Takeda[15] discussed the ultrasonic Doppler method for velocity profile measurement in fluid dynamics and fluid engineering. Soong et al.[13] measured the solid concentration in a slurry column; they developed an ultrasonic transmission technique to measure the solid concentration in a gas-liquid-solid bubble column reactor. Their results showed that the transit time could be correlated to the solid concentration, however their method could only measured the average solid concentration between the transmitter and the receiver. Carlson and Grenberg[4] proposed a method to measure the solid concentration in a multiphase flow with pulsed ultrasound based on the changes of the received energy slope. They used two small receivers and correlated the solid concentration to the average energy ratio received by the two receivers, and found a linear relationship within the solid mass fraction range 3%–15%. But for the concentrations below 3%, their method could not give accurate results. Bröring et al.[2] and Camarasa et al.[3] used the ultrasound Doppler technique to measure the bubble rise velocity, whereas the determination of the Doppler angle was questionable. Stolojanu and Prakash[14] investigated the feasibility of measuring concentrations of solids and bubbles in two-and three-phase systems. Their results show that in liquid-solid system both transmission time and amplitude ratio varies systemically with solid concentration. In presence of gas bubbles the variation of transmission time is not very regular while the relationship between attenuation of sound and phase holdups remain systematic.

Generally, two configurations are used in the literature, namely pitch-and-catch and pulse-echo configurations[1]. In the investigations reviewed above, all the reported measurements of the phase holdup adopted the pitch-and-catch configuration and plug-in manner, while the pulse-echo which can be used in a non-intrusive manner, is mainly limited to the velocity measurement. So development of measuring methods for the phase holdup and the phase velocity simultaneously with a pulse-echo ultrasound sensor is a valuable work.

Commercial Doppler ultrasound velocimetry is available, but it only provides limited function of measuring particle velocity in a liquid-solid system. If the particle size is small enough, this velocity can be considered as the liquid velocity. A commercial device Doppler ultrasound velocimetry DOP2000 is used in our investigation.

This work aims to extend its application to multiphase flows, developing ultrasound methods to measure the solid holdup in a liquid-solid system non-intrusively and to measure the liquid and bubble velocities simultaneously in gas-liquid system. Our investigation shows that the attenuation coefficient of the received echo energy monotonously increases with the increase of solid concentration, providing a method to measure the solid concentration. A model based on the ultrasound reflection and refraction law predicts the received echo energy in a good agreement with the experimental results. To measure the bubble behavior in gas-liquid or gas-liquid-solid system, it is commended to place the sensor probe in the flow direction in order to avoid the difficulty of determination of the Doppler angle. This work shows that the ultrasound Doppler velocimetry has powerful potential for mapping the flow field and phase structure in multiphase flow.

4.1.2.2 Algorithm and modeling

(1) Principle of Doppler ultrasound method

DOP2000 measures the particle velocity using the Doppler effect. When the ultrasound probe emits an ultrasound beam, the moving particles scatter the ultrasound wave. Partial backscattered ultrasound is then received by the same sensor probe. The movement of the particle subjects the received ultrasound to a frequency shift proportional to the particle velocity, as shown in Fig. 1. The frequency of the ultrasound perceived by the moving particles is

$$f_p = f_e - \frac{f_e \mid \boldsymbol{u}_p \mid \cos\theta}{c} \tag{1}$$

and the frequency of the ultrasound received by the stationary sensor probe is

$$f_r = \frac{c}{c + \mid \boldsymbol{u}_p \mid \cos\theta} f_p \tag{2}$$

Combination of Eqs. (1) and (2) and considering that $|\boldsymbol{u}_p|$ is usually much less than c yields

$$f_d = f_e - f_r \approx \frac{2 f_e \mid \boldsymbol{u}_p \mid \cos\theta}{c} \tag{3}$$

From the received echo signal the Doppler frequency is estimated and then the particle velocity is calculated using Eq. (3).

(2) Determination of Doppler angle

Accurate determination of the Doppler angle is a key problem for the Doppler ultrasound velocimetry application. It should be pointed out that the Doppler angle in Eq. (3) refers to the angle θ between the particle velocity and the ultrasound beam, not the angle α between the

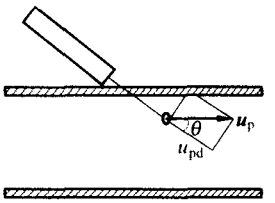

Fig. 1 Doppler effect caused by the moving particle

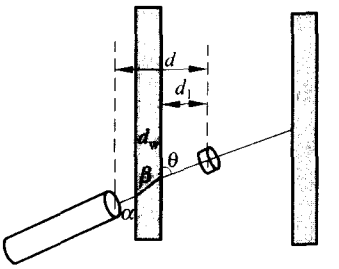

Fig. 2 Determination of the measuring location taking into account the ultrasound refraction and ultrasound velocity difference

probe and the column wall, as shown in Fig. 2. The relationship between α and θ can be determined based on the ultrasound refraction law. Similar to the light refraction law, the following two equations hold for the refraction at the outside and the inside interface of the wall, respectively,

$$\frac{c_c}{c_w} = \frac{\cos\alpha}{\cos\beta} \tag{4}$$

$$\frac{c_w}{c_l} = \frac{\cos\beta}{\cos\theta} \tag{5}$$

Combination of Eqs. (4) and (5) yields

$$\cos\theta = \frac{c_l}{c_c}\cos\alpha \tag{6}$$

where the ultrasound velocity c and the sensor placing angle α can be measured. Therefore, the Doppler angle can be determined by Eq. (6). The coupling media we used is ultragel with ultrasound velocity about 1500 m/s, very close to that in the water, so when the liquid is water, the difference between α and θ can be ignored. However, when the liquid has an ultrasound velocity quite different from that in ultragel, take olefin as an example, it is absolutely necessary to consider the difference between the sensor placing angle and the Doppler angle.

(3) Treatment of Doppler angle in turbulent flow

In a laminar flow, the tracer particle velocities remain constant both in amplitude and in direction, so the Doppler angle is invariant and easy to determine by Eq. (6). While in a turbulent flow, the turbulence makes the instantaneous Doppler angle time-dependent and almost impossible to determine. Here we make some discussions about the time-averaged Doppler angle. For a fully developed turbulent flow in a vertical tube, the instantaneous velocity can be denoted by

$$\boldsymbol{u}_p = (\bar{u} + u')\mathbf{i} + v'\mathbf{j} + w'\mathbf{k} \tag{7}$$

where u', v', and w' are the fluctuating velocity in the directions **i**, **j**, and **k**, respectively. Only the projection of $\boldsymbol{u}_p$ in the direction of the ultrasound beam u_{pd} influences the Doppler

frequency. Referring to Fig. 3, u_{pd} can be determined by

$$u_{pd} = u\cos\theta + v\sin\theta = |\boldsymbol{u}_p|\cos(\theta - \psi) \quad (8)$$

and the average Doppler frequency follows:

$$\bar{f}_d = \frac{2f_e\bar{u}_{pd}}{c} = \frac{2f_e\bar{u}\cos\theta}{c} \quad (9)$$

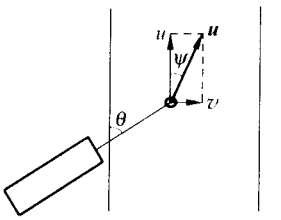

Fig. 3 Projection of the instantaneous particle velocity in the direction of the ultrasound beam

Eq. (9) shows that the fluctuating velocities in **j** and **k** directions have no influence on the time-averaged Doppler frequency; therefore the average axial velocity can be calculated by replacing the time-dependent Doppler frequency by time-averaged Doppler frequency. This can be realized by averaging enough velocity profiles.

(4) Determination of measuring location

DOP2000 is a non-intrusive device and the probe is fixed onto the plexiglass tube with a coupling media. In this case an ultrasound beam passes through media with different ultrasound velocities: the coupling media from the probe to the tube wall, with c_c; the tube wall medium, with c_w; and the liquid flowing in the tube, with c_l, as shown in Fig. 2. In a pulse-echo ultrasound probe, ultrasound waves are pulsed continuously. Immediately after emitting a pulse, the system is then switched to the receiving mode. At specific time increments Δt_i the echoes backscattered from the particles are detected for a time span dt ($dt \ll \Delta t_i$), i.e. from Δt_i to $\Delta t_i + dt$ so the measuring volume is a cylindrical slab of diameter d (approximately the same as the probe diameter) and height $h = c_l dt$. Referring to Fig. 2, the time interval Δt_i can be expressed as

$$\frac{\Delta t_i}{2} = t_c + t_w + t_l = \frac{d_c/\sin\alpha}{c_c} + \frac{d_w/\sin\beta}{c_w} + \frac{d_l/\sin\theta}{c_l} \quad (10)$$

In the commercial software provided with the DOP2000 equipment, the ultrasound refraction at the interface and the ultrasound velocity difference in different media are not considered, as shown in Fig. 4. The following equation is used in the commercial software:

$$\frac{\Delta t_i}{2} = \frac{d_c + d_w + d_l'}{c_l \sin\alpha} \quad (11)$$

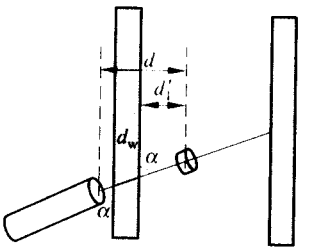

Fig. 4 Determination of the measuring location without taking into accounts the ultrasound refraction and ultrasound velocity difference

Therefore, the commercial software calculates the location of the measuring volume d incorrectly as d':

$$d' = d_c + d_w + d_l' = \frac{1}{2}c_l\Delta t_i \sin\alpha \quad (12)$$

However, Eq. (8) provides the time information Δt_i. Substituting Δt_i into Eq. (7) yields

$$d = d_c + d_w + d_l$$
$$= d_c + d_w + \left(\frac{d'}{c_l \sin\alpha} - \frac{d_c}{c_c \sin\alpha} - \frac{d_w}{c_w \sin\beta} \right) c_l \sin\theta \tag{13}$$

Thus, the correct measuring location can be obtained by modifying the DOP2000 calculated value through Eq. (13). Fig. 5 demonstrates the difference between the measuring location calculated by the DOP2000 software and by modifying Eq. (13). The difference between the two values is dependent on the ultrasound velocities in the coupling media, the wall material and the liquid. The larger is the difference among c_l, c_c and c_w, the larger is the difference between d and d_l'.

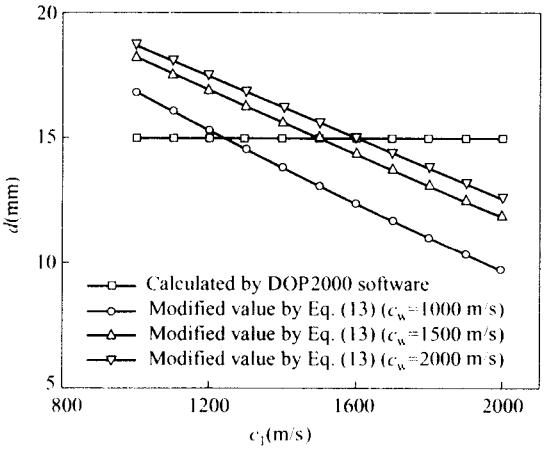

Fig. 5 Comparison between the calculated measuring location by Doppler software and by Eq. (13) under different ultrasound velocity in the wall material (c_c = 1500 m/s, d_0 = 2 mm, d_w = 5 mm)

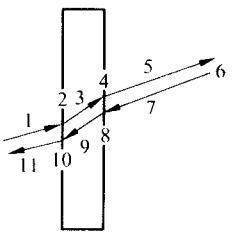

Fig. 6 Processes involved during the ultrasound emission and receiving

Notice that the measuring volume has limited dimensions and the measuring location is associated with the center of the measuring volume, special modification should be made to the near-wall region, Wunderlich and Brunn[23] made detailed discussion on the near-wall effect and proposed a modification model.

(5) Solid concentration measurement and modeling

In pulse-echo manner, the received echo energy is mainly influenced by the emission power, the solid concentration and the distance from the measuring volume to the probe. During the ultrasound emission and receiving, the following processes are involved, as shown in Fig. 6:

① Propagation in the coupling media.

② Refraction and reflection at the interface of the outside wall.

③ Propagation in the wall material.

④ Refraction and reflection at the interface of the inside wall.

⑤ Propagation in the fluid.

⑥ Backscattered by the particles.

⑦–⑪ Receiving the backscattered ultrasound by the same sensor through processes similar to ①–⑥.

Table 1 Variations of the ultrasound intensity in processes involved during ultrasound emission and receiving

$\frac{I_1}{I_0}=\exp(-\alpha_c s_c)$	(14)
$\frac{I_2}{I_1}=\zeta_1\frac{4Z_cZ_w}{Z_c^2+Z_w^2}$	(15)
$\frac{I_3}{I_2}=\exp(-\alpha_w s_w)$	(16)
$\frac{I_4}{I_3}=\zeta_3\frac{4Z_lZ_w}{Z_w^2+Z_l^2}$	(17)
$\frac{I_5}{I_4}=\exp[-\alpha_l(\varepsilon_s)s_l]$	(18)
$\frac{I_6}{I_5}=k_{bs}(\varepsilon_s)$	(19)
$\frac{I_7}{I_6}=\exp[-\alpha_l(\varepsilon_s)s_l]$	(20)
$\frac{I_8}{I_7}=\zeta_7\frac{4Z_wZ_l}{Z_w^2+Z_l^2}$	(21)
$\frac{I_9}{I_8}=\exp[-\alpha_w s_w]$	(22)
$\frac{I_{10}}{I_9}=\zeta_9\frac{4Z_cZ_w}{Z_c^2+Z_w^2}$	(23)
$\frac{I_{11}}{I_{10}}=\exp(-\alpha_c s_c)$	(24)

In a homogeneous liquid-solid system, the variations of the ultrasound intensity in each process are expressed in Table 1[1], where α_c, α_w and α_l are the attenuation coefficients of the coupling media, the wall material and the fluid, respectively, Z_c, Z_w, and Z_l are acoustic impedances, and $k_{bs}(\varepsilon_s)$ is the backscatter coefficient, which is dependent on the solid concentration. In Eqs. (15), (17), (21) and (23), ζ is the modifying coefficient of oblique incidence to the normal case, which is constant when the incident angle is invariant. Among the parameters involved in Eqs. (14)–(24), only α_l and k_{bs} are dependent on the solid concentration. Therefore, combination of Eqs. (14)–(24) yields the relationship between the emitted and the received ultrasound intensity: